Acta Cryst. (1993). B49, 223–235

Estimation of Ionicity Coefficients in Li_2BeF_4 Crystals by X-ray Diffraction

BY PAUL SEILER

Organic Chemistry Laboratory, Swiss Federal Institute of Technology, ETH-Zentrum, CH-8092 Zürich, Switzerland

(*Received* 20 *May* 1992; *accepted* 8 *September* 1992)

Dedicated to Professor Jack D. Dunitz on the occasion of his 70th birthday

Abstract

Ionicity coefficients of the atoms in lithium tetrafluoroberyllate (Li_2BeF_4) crystals have been estimated from accurate X-ray diffraction experiments at 81 K, using two different approaches. One is based on a series of least-squares calculations, in which the deviance $Q = \sum w(I_o - I_c)^2$ for model-sensitive low-order reflections is evaluated for different procrystal models; the other is based on partitioning of the deformation density. Ionicity coefficients p ($p = 1$ for neutral; $p = 0$ for ionic) based on Q values are about 0.8, 0.7 and 0.6 for Be, F and Li atoms, respectively. The corresponding net charges based on deformation-density maps (Hirshfeld partitioning scheme) are about +0.16, −0.09 and +0.11 e. However, these charge values do not yield the ionicity coefficients of individual atoms directly because the observable charge transfer between cationic and anionic components is reduced by overlap of neighboring atom densities. The reduction of charge transfer has been assessed from model calculations, *i.e.* difference maps were made by subtracting a neutral-atom promolecule density from a purely ionic one. The resulting (apparent) net charges are less than 25% of the formal ionic charge values (Be^{2+}, Li^+, F^-). When the reduction of charge transfer is taken into account, ionicity coefficients estimated in real space are about 0.6, 0.5 and 0.4 for Be, F and Li atoms, respectively. The bias of the results, produced by systematic errors such as extinction, scan truncation or exclusion of weak reflections is also discussed in some detail. Crystal data at 81 K: rhombohedral, $R\bar{3}$, hexagonal setting, $a = b = 13.281$ (2), $c = 8.888$ (1) Å, $V = 1357.7$ Å^3, $Z = 18$, $D_x = 2.18$ g cm^{-3}, μ(Mo $K\alpha$) = 2.09 cm^{-1}.

Introduction

For various ionic solids (*e.g.* LiH, LiF, NaCl *etc.*) X-ray diffraction has been applied in attempts to estimate the extent of charge transfer between atoms. Most of these studies are based on structure refinements, *i.e.* it was examined whether observed reflection intensities (especially of model-sensitive low-order reflections) agree better with those calculated for a neutral-atom or with those for an ionic procrystal model. The results have generally been inconclusive or at least incomplete.

One basic problem with this method is that the scattering factors of neutral atoms and their corresponding ions differ significantly only at small scattering angles. Hence, the smaller the unit cell, the smaller the number of observable model-sensitive reflections. Indeed, for LiH and LiF there are only two reflections with $H = 2\sin\theta/\lambda < 0.5$ Å^{-1}! Moreover, low-order reflections often suffer from large systematic errors such as extinction, multiple scattering, higher harmonic and nonlinear background contributions. Additional problems are connected with the refinement procedure itself, *e.g.* with the least-squares weights and the choice of the crystal models.

Information about the ionicity of ionic solids can of course also be obtained in real space, *e.g.* by integrating the electron density or deformation density associated with individual atoms. One essential deficiency of this method is that the charges (q) derived in this way depend strongly on the partitioning method used. In fact, several authors (see, for example, Catlow & Stoneham, 1983) have concluded that atomic charges cannot be established from experimental or theoretical charge-density studies because any partitioning of the charge density into ionic components is essentially arbitrary. Apart from the fact that the derived charges differ from one partitioning method to another, there are additional problems that are often ignored. Firstly, the apparent atomic charge (based on difference maps) is reduced by overlap of neighboring atom densities. Secondly, the charge distribution of the reference atoms, neutral or ionic, extends to infinity, while most charge-transfer estimates in a solid involve a finite partitioning of the space surrounding the atoms. In this sense, the maximum observable charge transfer (hereafter denoted as q_0) between cationic and anionic components is always smaller than formal ionic charge values (*e.g.* Li^+, F^-). In the

0108-7681/93/020223-13$06.00

present analysis, q_0 has been assessed *via* model-difference maps by subtracting a neutral-atom promolecule density from a purely ionic one (and *vice versa*); ionicity coefficients p of individual atoms were then evaluated from the ratio q/q_0.

Li_2BeF_4 is certainly not a prototype of an ionic compound. Nevertheless, it is an ideal test compound because there are some 40 model-sensitive reflections in the low-order region with $H < 0.5$ Å^{-1} (and ~ 120 reflections with $H < 0.73$ Å^{-1}), which can be used, in principle, to determine ionicity coefficients in reciprocal space. Moreover, deformation-density maps of high quality can be obtained from these crystals.

We are aware, of course, that the atomic charge is strictly a nonmeasurable quantity and that the results given in this paper have a certain degree of arbitrariness, depending on the choice of the partitioning method. Still, it has been shown in several studies (see, for example, Maslen & Spackman, 1985) that such charge estimates can be very useful for explaining various chemical and physical properties of molecules and solids.

Previous work on the Li_2BeF_4 structure

Zachariasen (1926) concluded from powder photographs that Li_2BeF_4 is isomorphous with phenacite, Be_2SiO_4, the structure of which was determined partially by Bragg (1927) and then completely solved by Bragg & Zachariasen (1930). The isomorphism of Li_2BeF_4 and phenacite was confirmed by Hahn (1954) from single-crystal studies and the structure of the former was then refined in a detailed study of Burns & Gordon (1966). In this rhombohedral structure (space group $R\bar{3}$), each Li and Be atom is surrounded by a tetrahedron of F atoms and each F atom has one Be and two Li atoms as nearest neighbors; chains of interlinked tetrahedra run along the c axis of the corresponding hexagonal cell (Fig. 1). The crystal structure and lattice energy can be reproduced extremely well by force-field calculations based on a purely ionic model (Busing, 1972), although McGinnety (1973) considers that covalent interactions, especially along Be—F bonds, are not negligible. A deformation-density study by Collins, Mahar & Whitehurst (1983) based on room-temperature X-ray data indeed showed appreciable bonding density (~ 0.42 e Å^{-3}) along Be—F bonds and much weaker density along Li—F bonds, supporting the presumed partial covalent character of these bonds. It was this latter result that roused our attention, since we had found much lower peak heights (~ 0.1 e Å^{-3}) along C—F bonds in two organic molecules (Dunitz, Schweizer & Seiler, 1983) and it seemed unlikely to us that Be—F bonds should be more covalent than C—F bonds. Since inadequate atomic displacement parameters can lead to spurious features in difference-density maps, we decided to examine the difference density of Li_2BeF_4 from low-temperature (81 K) X-ray data (Seiler & Dunitz, 1986*a*).

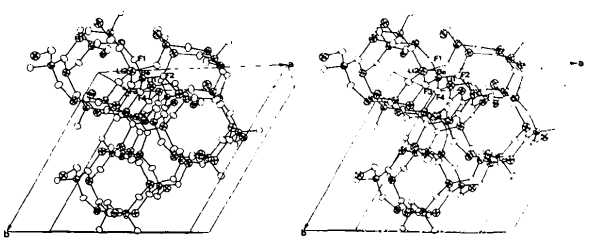

Fig. 1. Stereoview of the crystal packing of Li_2BeF_4. The atomic displacement ellipsoids are based on data set 1 (81 K) and are drawn at the 98% probability level.

In our earlier analysis we reached two main conclusions. Firstly, that deformation densities based on a neutral-atom and an ionic procrystal model are very similar. Peak heights along Be—F and Li—F bonds based on all $F_o - F_c$ coefficients out to $H = 1.8$ Å^{-1} were about 0.2 and 0.08 e Å^{-3}, respectively, *i.e.* about half the values observed by Collins *et al.* (1983). Owing to a programming error, the contour interval in our first paper was stated to be three times lower than the real value; this was subsequently corrected in an erratum (Seiler & Dunitz, 1986*b*). Secondly, it was claimed that the charge density in this crystal is represented somewhat better as a superposition of spherical neutral-atom charge distributions than as a superposition of ionic charges. This result was derived from a series of least-squares calculations: the minimum of the deviance $Q = \sum w(I_o - I_c)^2$ for 22 model-sensitive reflections ($H < 0.5$ Å^{-1}), evaluated as a function of the ionicity coefficients (p), occurred close to the neutral-atom structure (see below). However, it was also pointed out by Seiler & Dunitz (1986*a*) that p coefficients of Li atoms are much less well determinable than those of Be and F atoms. In fact, with the approximations made at the time the results were not really conclusive for the highly diffuse Li atoms.

Since then, considerable efforts have been made to clarify this problem. Firstly, ionicity coefficients were re-estimated by the procedure described by Seiler & Dunitz (1986*a*) using more accurate and more extensive X-ray data. Secondly, atomic charges were derived from (dynamic) difference-density maps by application of the Hirshfeld partitioning scheme (Hirshfeld, 1977). Thirdly, model calculations were carried out to estimate the upper limit of the observable diffuse charge transfer between cationic and anionic components in these crystals. Fourthly, ionicity coefficients of individual atoms were estimated from difference-density maps. Fifthly, the

influence of several experimental factors such as extinction correction, scan truncation, series termination and exclusion of weak reflections in least-squares refinements or difference syntheses was investigated. Sixthly, the standard Hartree–Fock f curves listed in *International Tables for X-ray Crystallography* (1974, Vol. IV), used in this analysis, are compared with those of Hess, Lin, Niu & Schwarz (1993), in which electron correlation as well as the crystal-field correction in Li_2BeF_4 are considered; some results obtained from these new f curves are also reported.

Experimental

X-ray measurements were carried out with two Enraf–Nonius CAD-4 diffractometers equipped with graphite monochromators (Mo $K\alpha$ radiation, λ = 0.7107 Å) and a locally modified Enraf–Nonius gas-stream low-temperature device. The temperature of the gas stream was kept constant at about 81 K. Temperature fluctuations monitored by a Pt100 resistor were less than ± 0.3 K during the experiment.

X-ray data are based on three crystal specimens with diameters of about 0.42, 0.22 and 0.15 mm for crystals 1, 2 and 3, respectively. Unit-cell dimensions at 81 K were obtained by least-squares refinement of setting angles for 22 reflections with 2θ values in the range 90–100°. The values listed in the *Abstract* are based on measurements with crystal 1; corresponding values obtained from crystal 2 agree within one standard deviation.

Integrated relative intensities were measured by $\omega/2\theta$ scans. A variable scan angle was taken for the peak: $\Delta\omega = A + B\tan\theta$, plus a quarter of this scan angle at the scan limits for background measurements. The values of A and B, as well as the size of the counter aperture, were determined experimentally by analyzing the net intensity of 22 reflections ($0.2 < H < 2.7$ Å^{-1}) as a function of scan angle and counter aperture. The optimal values for A were found to be 1.4, 0.9 and 0.6° for crystals 1, 2 and 3, respectively; a B value of 0.7° was chosen for all three crystal specimens. For crystal 1, a vertical aperture of 0.8° was used up to $H = 2.4$ Å^{-1}; it was then increased successively with increasing scattering angle to reach a maximum value of 0.92° at H = 2.72 Å^{-1}. The horizontal aperture was 0.64° throughout. For measurements with crystals 2 and 3, both apertures were kept constant at 0.48°.

We now describe some specific details of data sets 1 (crystal 1, $0 < H < 2.72$ Å^{-1}) and 2 (crystal 2, $0 < H < 1.4$ Å^{-1}), used to determine atomic parameters and electron-density difference maps.

Six standard reflections, distributed over the measured H ranges, were monitored at intervals of 20 000 s radiation time. They showed a uniform slow intensity decrease amounting to about 5 and 3% at the end of the measurement periods (about 84 and 51 d) for crystals 1 and 2, respectively. The intensity loss, mainly caused by radiation damage, is practically independent of scattering angle and crystal orientation.

For data set 1, nearly all symmetry-equivalent reflections out to $H = 1.0$ Å^{-1} were measured in two crystal orientations (at ψ angles of ± 25°, mostly 12 equivalent measurements); then all accessible reflections out to $H = 2.72$ Å^{-1} were measured in one orientation, a total of about 40 000 measurements (6345 unique reflections). For data set 2, most symmetry-equivalent reflections were measured in two crystal orientations, a total of about 10 500 (877 unique) reflections. For both data sets, the 22 weakest low-order reflection intensities ($0 < H < 0.5$ Å^{-1}) were estimated from azimuthal intensity profiles to reduce multiple-scattering contributions as far as possible.

A rapid prescan (up to 40 s) was carried out to determine the optimal scan speed of weaker reflections. Only those reflections for which the relative precision $[\sigma(I_o)/I_o]$ was larger than 0.015 were rescanned. For reflections scanned twice, both scan rates were added to avoid a systematic bias in I_o (for details see Seiler, Schweizer & Dunitz, 1984). The maximum scan time (including prescan time) to reach the desired precision was 340 and 640 s for data sets 1 and 2, respectively. Individual intensity measurements were normalized to a standard scan speed, corrected for isotropic absorption and for the slow intensity drift. After elimination of large multiple-scattering contributions, equivalent reflections were averaged to give mean intensities. The internal agreement $R_{\rm int} = (\sum_H \sum_{i=1}^N |I_{H,i} - \langle I_H \rangle|)/\sum_H N\langle I_H\rangle$ is 0.015 and 0.013 for data sets 1 and 2, respectively. Data set 2 was completed by adding the high-order data of crystal 1 ($1.4 < H < 2.72$ Å^{-1}) to the (scaled) low-order data ($0 < H < 1.4$ Å^{-1}) of crystal 2. $R_{\rm int}$ among data sets 1 and 2, based on all 877 scaled (mean) intensities ($0 < H < 1.4$ Å^{-1}) is 0.026; without the 30 strongest reflections it is 0.005.

Standard deviations $\sigma(I_o)$ of mean intensities were estimated from counting statistics, SIGSTAT = $[\sum_i (p_i + 4b_i + 0.0002I_i^2)]^{1/2}/N$ (where p_i and b_i are respectively the normalized peak and background variances for individual measurements), as well as from the deviations of individual measurements from their respective means, SIGDEV = $[\sum_{i=1}^N (I_i - \langle I\rangle)^2/N(N-1)]^{1/2}$. For data sets 1 and 2, we used the larger of the two estimates. Atomic parameters and interatomic distances listed in Tables 1 and 2 refer to data set 1.

The scan-truncation error introduced by our measurement procedure should be smaller than 5% at

Table 1. *Positional and displacement parameters* (Å^2) (*all* $\times 10^5$ *with e.s.d.'s in parentheses*) *based on data set* 1 (81 K)

All 6345 measured reflections included out to $H = 2.72$ Å^{-1}. The first line refers to neutral-atom scattering factors *N*1, the second line to ionic scattering factors *I*1. Displacement parameter expression: $T = \exp(-2\pi^2 h_i a^i U_{ij} h_j a^j)$.

	x	y	z	U_{11}	U_{22}	U_{33}	U_{12}	U_{13}	U_{23}
F(1)	10542 (1)	−11059 (1)	25185 (1)	575 (1)	536 (1)	609 (1)	113 (1)	−9 (1)	25 (1)
	10541 (1)	−11058 (1)	25185 (1)	581 (1)	542 (1)	615 (1)	116 (1)	−9 (1)	25 (1)
F(2)	32333 (1)	563 (1)	24887 (1)	512 (1)	604 (1)	770 (1)	303 (1)	−20 (1)	−25 (1)
	32334 (1)	563 (1)	24887 (1)	518 (1)	609 (1)	775 (2)	306 (1)	−20 (1)	−25 (1)
F(3)	20410 (1)	7550 (1)	10393 (1)	905 (1)	646 (1)	460 (1)	470 (1)	−8 (1)	54 (1)
	20410 (1)	7550 (1)	10393 (1)	911 (2)	651 (1)	466 (1)	473 (1)	−7 (1)	54 (1)
F(4)	20938 (1)	8201 (1)	39282 (1)	924 (1)	692 (1)	470 (1)	510 (1)	−25 (1)	−76 (1)
	20938 (1)	8201 (1)	39283 (1)	930 (2)	697 (1)	475 (1)	514 (1)	−25 (1)	−75 (1)
Be	21175 (1)	1535 (1)	24950 (1)	609 (3)	563 (3)	531 (3)	294 (2)	−10 (2)	−48 (2)
	21175 (1)	1535 (1)	24949 (2)	588 (3)	542 (3)	513 (3)	284 (3)	−10 (3)	−56 (2)
Li(1)	21476 (2)	2096 (2)	58178 (3)	921 (7)	871 (7)	790 (7)	455 (6)	210 (5)	−13 (5)
	21474 (2)	2096 (3)	58176 (3)	914 (8)	867 (7)	786 (8)	448 (6)	239 (6)	−10 (6)
Li(2)	20754 (2)	1644 (2)	−8496 (3)	892 (7)	840 (7)	798 (7)	438 (6)	5 (5)	14 (5)
	20759 (2)	1646 (2)	−8496 (3)	889 (8)	841 (7)	794 (8)	438 (6)	5 (6)	15 (6)

Table 2. *Interatomic distances* (Å) *at* 81 K (*with e.s.d.'s in parentheses*) *based on the positional parameters obtained from neutral-atom scattering factors*

Be—F(1)	1.5590 (2)	Li(1)—F(1′)	1.8511 (2)	Li(2)—F(1′)	1.8645 (2)
Be—F(2)	1.5505 (2)	Li(1)—F(2′)	1.8594 (2)	Li(2)—F(2′)	1.8461 (2)
Be—F(3)	1.5503 (2)	Li(1)—F(4)	1.8817 (3)	Li(2)—F(3′)	1.8537 (2)
Be—F(4)	1.5606 (2)	Li(1)—F(4′)	1.8887 (2)	Li(2)—F(3)	1.8633 (3)

$H_{max} = 2.72$ Å^{-1}. In fact, since no thermal diffuse scattering (TDS) correction was applied we cannot exclude the possibility that the net intensity of highest-order reflections is somewhat overestimated. The analysis of the tails of the reflection profiles as a function of scattering angle, scan angle, counter aperture and temperature (for details of the method see Seiler, 1992) indicate that TDS contributions at 81 K are small but not negligible.

To estimate the effect of scan truncation on our results (see later section on systematic errors) we introduced an artificial truncation error in data set 1 (hereafter denoted as data set 1 mod), amounting to about 5% at H_{max}. A similar error would occur with a standard measuring procedure, in which the increase of $\Delta\omega$ is based on a B value of 0.35 instead of 0.7.

Data set 3 ($0 < H < 0.73$ Å^{-1}) was used to determine ionicity coefficients in reciprocal space. This is based on the low-order intensities of data sets 1 and 2, and on three additional measurements (one for each crystal specimen) carried out on a second diffractometer that was equipped with a nearly perfect graphite monochromator. The measurement procedure was the same as described for data sets 1 and 2. For each crystal specimen, symmetry-equivalent reflections ($0 < H < 0.73$ Å^{-1}) were measured in at least two crystal orientations (at ψ angles of $\pm 25°$), a total of about 1500 (122 unique) reflections. For the weakest reflections ($H < 0.5$ Å^{-1}), azimuthal intensity profiles were recorded to reduce multiple-scattering contributions. The intensity loss of standard reflections, observed at the end of individual measurement periods, was less than 1% and was compensated in the usual way. The final data set was produced as follows. Strong reflections with estimated $y = I_o/I_{kin}$ values < 0.99 were eliminated. Then, the five individual (scaled) intensity measurements, corrected for various systematic errors (including extinction) were averaged [$R_{int} = 0.005$ for the remaining 102 unique reflections; note that I_o and $\sigma(I_o)$ for the three strongest reflections are based only on measurements with crystals 2 and 3]. The strongest reflection intensities ($H < 0.5$ Å^{-1}, listed later in Table 5*a*), are almost the same as those tabulated in our original paper (Seiler & Dunitz, 1986*a*), whereas the weakest ones ($I_o < 350$) changed significantly (by up to 4%). Moreover, standard deviations (SIGDEV values) of the weakest reflections increased markedly.*

Results from two-dimensional intensity measurements

For 18 model-sensitive low-order reflections ($H < 0.44$ Å^{-1}) of crystal 1, I_o was also evaluated from two-dimensional $\Delta\omega$, $\Delta 2\theta$ intensity measurements at 81 K, using a narrow vertical slit (0.1 × 5 mm) in

* Lists of structure factors have been deposited with the British Library Document Supply Centre as Supplementary Publication No. SUP 55550 (45 pp.). Copies may be obtained through The Technical Editor, International Union of Crystallography, 5 Abbey Square, Chester CH1 2HU, England.

front of the detector (details will be published elsewhere). The advantages of such a procedure have been discussed in detail by Mathieson (1982, 1984, 1988). Application of this method requires high stability of the experimental setup, especially when working at low temperatures. Moreover, it can be extremely time-consuming: for example, the time spent in measuring the weakest reflection intensity to a relative precision of 0.3% was about 8 h. Thus, only two equivalent reflections were measured, although in a crystal orientation where multiple-scattering contributions should be minimal. Table 5(*a*) shows that I_o values obtained from conventional one-dimensional measurements and corresponding two-dimensional measurements agree mostly within 1.5%; for the four weakest reflections ($I_o < 590$), two-dimensional measurements yield slightly higher intensities (up to 5%). Inspection of one-dimensional (ω and $\omega/2\theta$ scans) and two-dimensional intensity profiles indicate that the weakest reflections could be contaminated by the tails of strong neighboring reflections. This could be tested by remeasuring the intensities of these reflections with a highly monochromatic X-ray beam, obtainable, for example, from a double-crystal spectrometer. Note that during irradiation of crystals 1 and 2 the intensity of the weak 003 reflection (contaminated by 006, the second strongest reflection) increased by several per cent; thus 003 was discarded from data set 3.

Structure refinements

A series of least-squares refinements was carried out with data sets 1 and 2, using different procrystal models, inclusion criteria of reflections, extinction models *etc.* Only a summary of the results obtained with data set 1 is given here, since atomic parameters obtained with data set 2 agree mostly within 1–2 e.s.d.'s. The residuals $\sum w(I_o - I_c)^2$ were minimized by a full-matrix least-squares method [$w = 1/\sigma(I_o)^2$] with programs *CRYLSQ*, implemented in the *XRAY* system (Stewart, Kruger, Ammon, Dickinson & Hall, 1972) and in *XTAL* 3.0 (Stewart & Hall, 1990). Scattering factors for neutral atoms and ions, as well as dispersion corrections (considered only for F atoms) were taken from *International Tables for X-ray Crystallography* (1974, Vol. IV). The shift/e.s.d. ratios of the refined parameters were smaller than 10^{-4}. From now on, neutral-atom and ionic scattering factors (and corresponding crystal models) are denoted as *N*1 and *I*1, respectively.

The positional parameters based on data set 1 (including all 6345 measured reflections out to $H = 2.72$ Å^{-1}) are almost the same for the two extreme procrystal models (see Table 1). The changes in the atomic displacement parameters are very small but show systematic behavior. From *N*1 to *I*1, the average change in U_{ii} components is about 6×10^{-5}, -20×10^{-5} and -4×10^{-5} Å^2 for F, Be and Li atoms, respectively.

Table 3. *Selected results obtained from the I refinements of data set* 1 (81 K)

*N*1, *N*1(*H*) and *I*1 refer to neutral-atom and ionic crystal models at the self-consistent-field level. Displacement parameters (Å^2) all $\times 10^5$. Definitions: $S(I) = [\sum w(I_o - I_c)^2/(N_{obs} - N_{var})]^{1/2}$; $R(F) = \sum(||F_o| - |F_c||)/\sum|F_o|$; $wR(F) = [\sum w(|F_o| - |F_c|)^2/\sum wF_o^2]^{1/2}$; $R(I) = \sum(|I_o - I_c|)/\sum I_o$; the isotropic extinction parameter g refers to a type 1 model with Lorentzian mosaic-spread distribution; $y = I_o/I_{kin}$. E.s.d.'s are given in parentheses.

		*N*1	*N*1(*H*)	*I*1
F(1)	U_{11}	575 (1)	577 (1)	581 (1)
	U_{22}	536 (1)	537 (1)	542 (1)
	U_{33}	609 (1)	608 (2)	615 (1)
Be	U_{11}	609 (3)	602 (3)	588 (3)
	U_{22}	563 (3)	559 (3)	542 (3)
	U_{33}	531 (3)	526 (3)	513 (3)
Li(1)	U_{11}	921 (7)	899 (9)	914 (7)
	U_{22}	871 (7)	866 (8)	867 (7)
	U_{33}	790 (7)	786 (9)	786 (7)
$2\sin\theta/\lambda$ range (Å^{-1})		0–2.72	2.0–2.72	0–2.72
N_{obs}		6345	3810	6345
Scale factor		1.0000 (5)	0.9998 (14)	1.0076 (5)
$g \times 10^{-4}$		0.18 (1)	0.18	0.24 (1)
y_{min}		0.74	-	0.68
$S(I)$		1.52	1.14	1.69
$R(F)$		0.015	0.020	0.015
$wR(F)$		0.013	0.013	0.015
$R(I)$		0.022	0.017	0.017

A high-order refinement based on the neutral-atom model was also carried out, including all 3810 measured reflections with $H > 2.0$ Å^{-1} [see *N*1(*H*) of Table 3]. The positional parameters (not listed) and the U_{ij} values of F atoms are almost the same as those obtained from all observations (*N*1); relative to *N*1, the U_{ii} components of Be atoms decrease by about 5×10^{-5} Å^2 on average, those of Li atoms by about 7×10^{-5} Å^2. In view of these small differences, deformation-density maps are based on atomic parameters obtained from full-data refinements.

The atomic parameters listed in Table 1, in particular the U_{ij} values, are much less accurate than their precision estimates (see e.s.d.'s in parentheses) suggest; the U_{ij} values are clearly model dependent and also sensitive to systematic errors in the data. For example, a small systematic bias in I_o due to scan truncation or neglect of TDS contributions could change the U_{ij} values in one or the other direction by several per cent. When the refinements are repeated with data set 1 mod, in which an artificial scan-truncation error is introduced (see *Experimental*), comparable U_{ii} components increase by about 5%.

Selective exclusion of weak reflections

Hirshfeld & Rabinovich (1973) have argued that selective exclusion of weak (or negative) intensities from least-squares refinement leads to a bias in the

remaining observations towards too high F^2 (or I) values and thus to systematic errors of the refined parameters. Although the arguments against rejection of weak reflections are accepted in principle, the resulting errors introduced by such practices are in general less severe than sometimes claimed. For example, in the X-ray analysis of tetrafluoroterephthalonitrile (TFT) at 98 K (Seiler *et al.*, 1984), exclusion of more and more weak reflections from high-order refinements led to physically insignificant changes in the atomic parameters and the scale factor. However, there was also some criticism of the analysis. One of the referees of the paper pointed out that the weakest high-order reflection intensities were obtained from (too) rapid prescan measurements and that their actual least-squares weights were too small to detect such a bias.

In the present analysis, the problem was taken up again, since the high-order data of data set 1 are at least an order of magnitude more precise (and more accurate) than those obtained for TFT. As in the previous study, a series of high-order refinements was made, beginning with all 3810 reflections [$2.0 < H < 2.72$ Å^{-1}, $R(I) = 0.017$]; then the reflections with $I_o < 10\sigma(I_o)$, $I_o < 20\sigma(I_o)$ up to $I_o < 70\sigma(I_o)$ were successively excluded, until only 384 reflections remained [$R(I) = 0.006$]. The 63 atomic parameters and the scale factors obtained from these refinements did not change more than about one standard deviation, and no systematic bias of the atomic parameters was observed. In fact, all 64 parameters refined to consistent values when only the 70 strongest high-order reflections were included!

Extinction correction

The kinematic intensity of a reflection can be estimated experimentally, *e.g.* by altering the crystal thickness and measuring the intensity for different path lengths of the X-ray beam and extrapolating to zero path length (Bragg, James & Bosanquet, 1921). For the present analysis, low-order reflections were measured for different path lengths, using the three nearly spherical crystal specimens (see *Experimental*). However, it was not possible to estimate extinction by this procedure because of unequal crystal perfection of the individual specimens. In fact, extinction (estimated from least-squares refinements) for crystal 3 (diameter ~ 0.15 mm) was slightly more severe than for crystal 2 (diameter ~ 0.22 mm). Azimuthal intensity profiles of the strongest reflections showed that extinction is only slightly anisotropic: *e.g.* for the strongest reflection of crystal 1 intensity fluctuations are within about 8%.

In the present anaiysis, isotropic extinction corrections are based on least-squares analyses, with use of the method of Becker & Coppens (1974) and the assumption of a Lorentzian mosaic-spread distribution. The results, summarized in Table 4 show that g, ρ and $y = I_o/I_{kin}$ values depend significantly on the actual crystal model used. For example, from the neutral-atom model $N1$ to the ionic model $I1$, y of the strongest reflection of crystal 1 changes from 0.74 to 0.68. Also, the classification of extinction in terms of type 1 and type 2 is not unequivocal. For the neutral-atom model, the type 2 correction gives slightly better R factors (for the seven strongest reflections) than the type 1 correction; for the ionic model, this is reversed. A mixed extinction type was also considered for both crystal models but with unsatisfactory results: when the two extinction parameters were refined simultaneously, they did not converge. For crystal 2, extinction is severe only for two reflections with y values (based on $N1$) of about 0.86. Since none of these crystal or extinction models correspond to the 'true model', the kinematic intensities (at least for the very strongest reflections) ought to be determined experimentally, *e.g.* by using synchrotron radiation and a very small crystal specimen. The influence of different extinction-correction models on difference-density maps and atomic net charges is described in the later section on systematic errors.

Table 4. *Results of isotropic extinction corrections based on the formalism of Becker & Coppens* (1974), *with the assumption of a Lorentzian mosaic-spread distribution*

$N1$ and $I1$ refer to neutral-atom and ionic models at the SCF level and $R(F)$ refers to the seven strongest low-order reflections. E.s.d.'s of g and ρ values are given parentheses.

	Type 1		Type 2	
	$N1$	$I1$	$N1$	$I1$
Crystal 1 (81 K)				
$g \times 10^{-4}$	0.18 (1)	0.24 (1)		
$\rho \times 10^{-4}$			0.60 (3)	0.76 (3)
y_{min}	0.74	0.68	0.73	0.68
$R(F)$	0.012	0.005	0.010	0.020
Crystal 2 (81 K)				
$g \times 10^{-4}$	0.16 (1)	0.24 (1)		
$\rho \times 10^{-4}$			0.50 (3)	0.67 (3)
y_{min}	0.86	0.80	0.86	0.80
$R(F)$	0.013	0.007	0.007	0.008

Analysis of data

After least-squares refinements with data sets 1 and 2, the ratio I_o/I_c was analyzed as a function of scattering angle and I_o. The values given below refer to data set 1 and scattering factors $N1$ and $I1$ (values in parentheses). The reflection sphere, including all 6345 observations, was divided into 14 shells (from $0 < H < 0.2$ Å^{-1} up to $2.6 < H < 2.72$ Å^{-1}). Then, for each shell, a scale facor $S = \sum I_o/\sum I_c$ was calculated for various ranges of I_o. With consideration of all

observations, S has a maximum of 1.026 (1.032) for the shell $0.2 < H < 0.4$ Å^{-1}; for shells with $H >$ 1.2 Å^{-1}, S varies between -0.997 (-0.997) and 1.004 (1.006). However, for weak reflections alone (I_o < 100), S is significantly larger than unity, *i.e.* the weak reflection intensities appear to be overestimated. For very weak reflections with $I_o < 40$, S is about 1.2 and 1.06 for the shells $1.0 < H < 1.2$ and $2.6 < H < 2.72$ Å^{-1}, respectively. (Note that up to H = 0.6 Å^{-1} there are no reflections with $I_o < 40$ and up to $H = 1.0$ Å^{-1} there are only 9). This result may suggest that the data are still contaminated by multiple-scattering contributions and, in principle, an overall correction could be applied to compensate for this (Le Page & Gabe, 1979). About 50 of these weakest reflections with $I_o/I_c > 1.5$ were carefully remeasured at 81 K in many crystal orientations with crystal specimens 1 and 2. For comparable reflections, the (scaled) mean intensities, corrected for large multiple-scattering contributions, agree within about three e.s.d.'s, but with respect to their calculated intensities they are still considerably too high (by up to 50%). Thus, it would appear that this systematic bias must be related to additional factors such as TDS and higher-harmonic contributions of the incident radiation and possibly to inadequacy of the applied crystal models (spherical reference atoms, disorder, neglect of anharmonic vibration, incorrect phases). For the present analysis, all measured reflections were included in least-squares refinements; for deformation-density maps, the weakest reflections with $I_o < 40$ and $H > 1.0$ Å^{-1} were discarded.

Estimation of ionicity coefficients in reciprocal space

In a first step, least-squares calculations were carried out for the two extreme procrystal models *N*1 and *I*1 (with fixed atomic parameters given in Table 1 but with refinement of the scale factor and overall temperature factor) with use of the 102 weak accurately measured low-order reflection intensities ($0 < H <$ 0.73 Å^{-1}) of data set 3. The results, listed for the 26 lowest-order reflections ($H < 0.5$ Å^{-1}) in Table 5(*a*), clearly show that the observed intensities are much closer to those calculated from the neutral-atom model, in agreement with our first analysis. Note that, in contrast to the earlier analysis, the 110 reflection ($y \simeq 0.98$) and the 003 reflection (contaminated by the strong 006 reflection) have been discarded and six additional reflections (with $H <$ 0.5 Å^{-1}) have been included.

As a crude first approximation, the scattering factors for each type of atom can be represented as a linear combination of the neutral and charged species, *viz*

$$f(A) = p_A f(A^0) + (1 - p_A) f(A^{\text{ion}})$$

where the condition $2p(\text{Li}) + 2p(\text{Be}) = 4p(\text{F})$ is imposed to preserve electric neutrality of the crystal. The p coefficients can be determined, in principle, by least-squares analysis. What we have done is to calculate the deviance $Q = \sum w(I_o - I_c)^2$ for many different sets of p coefficients, ranging from the neutral-atom model ($p = 1$) to the ionic model ($p = 0$). The step size (Δp) from one set to the other was 0.1 for Be and Li atoms and 0.05 for F atoms. With data set 3, there is a minimum in Q close to $p(\text{Be}) \simeq 0.8$, $p(\text{F}) \simeq 0.7$ and $p(\text{Li}) \simeq 0.6$, *i.e.* the atoms appear to be more 'ionic' than reported in our first analysis. However, as seen from Table 5, the neutral-atom and hybrid models fit the observations almost equally well. In other words, the minimum towards the neutral-atom model is so flat that slight changes in the observations, the least-squares weights and the scale factor can cause considerable shifts in the optimal p values, especially p(Li). Inclusion of additional reflections (up to $H = 0.73$ Å^{-1}) makes the minimum even flatter because the calculated intensities become much less model dependent with increasing scattering angle. Indeed, for many of these reflections, I_c is almost invariant from one crystal model to another; inclusion of the additional reflections served mainly to stabilize the scale factor.

So far, the analysis was restricted to a small number of low-order reflections because f curves of neutral atoms and corresponding ions differ appreciably only at small scattering angles (up to $H \simeq$ 0.5 Å^{-1} for Li atoms and $\simeq 0.7$ Å^{-1} for Be and F atoms). Is there any point in extending the resolution? At larger scattering angles, the differences become so small that a tiny systematic bias in the data, in the crystal models or in both could lead to erratic results, especially for Li atoms. Nevertheless, we repeated the calculations described above including the 521 weakest reflections (with y coefficients > 0.995 and $H < 1.2$ Å^{-1}) measured with crystal 2. Best agreement was obtained close to $p(\text{Be}) \simeq 0.75$, $p(\text{F}) \simeq 0.55$ and $p(\text{Li}) \simeq 0.35$ but the minimum in Q is so flat that other sets of p coefficients, ranging from $p(\text{Be}) \simeq 0.80$ to 0.6, $p(\text{F}) \simeq 0.65$ to 0.4 and $p(\text{Li}) \simeq$ 0.45 to 0.2, give essentially the same result.

Electron-density difference maps and atomic net charges

The difference-density maps shown here are based on data sets 1 and 2 and on standard scattering factors listed in *International Tables for X-ray Crystallography* (1974, Vol. IV). Atomic net charges were obtained by partitioning the deformation density according to the stockholder recipe (Hirshfeld, 1977) *via* program *CHARGE* (*XTAL*3.0; Stewart & Hall, 1990). The integration is based on an atom range of 6 Å; the inclusion region, which encompasses contri-

Table 5. *Results for the neutral-atom model N1, the ionic model I1 and the hybrid model* $p(Be)\simeq 0.8$, $p(F)\simeq 0.7$, $p(Li)\simeq 0.6$

(*a*) Measured and calculated intensities for 26 weak model-sensitive low-order reflections

The observed values given first are mean intensities obtained from three crystal specimens [one-dimensional (1*D*) measurements, see data set 3]; the values in parentheses are based on crystal 1 [two-dimensional (2*D*) measurements] and are only listed for comparison.

				I_o		I_c		I_c $p(Be)\simeq 0.8$ $p(F)\simeq 0.7$ $p(Li)\simeq 0.6$		I_c	
h	*k*	*l*	$2\sin\theta/\lambda$	1*D*	2*D*	Neutral	ΔI		ΔI	Ionic	ΔI
1	0	1	0.142	962	(951)	946	16	964	−2	929	33
2	0	−1	0.208	716	(724)	757	−41	759	−43	549	167
1	0	−2	0.242	46404	(46319)	46979	−575	46880	−476	41697	4707
2	1	1	0.256	54502	(54482)	55181	−679	54784	−282	48538	5964
1	2	−1	0.256	77823	(77279)	79065	−1242	78396	−573	68628	9195
2	0	2	0.284	9990	(9937)	9860	130	9834	156	9174	816
1	2	2	0.322	13580	(13593)	13563	17	13367	213	12013	1567
2	1	−2	0.322	13929	(14143)	13803	126	13676	253	12575	1354
1	3	1	0.334	11061	(11144)	11054	7	10860	201	9695	1366
3	1	−1	0.334	590	(606)	629	−39	578	12	364	226
4	0	1	0.366	8858	(8841)	8526	332	8672	186	8981	−123
3	1	2	0.386	174	(184)	187	−13	183	−9	162	12
1	3	−2	0.386	77	(80)	76	1	71	6	51	26
3	2	1	0.396	3203	(3163)	3055	148	3124	79	3316	−113
2	3	−1	0.396	828	(836)	788	40	783	45	754	74
4	0	−2	0.414	174	(177)	163	11	133	41	54	120
2	3	2	0.440	11197	(11132)	10878	319	11133	64	11880	−683
3	2	−2	0.440	450		461	−11	466	−16	484	−34
5	0	−1	0.450	5082		4929	153	4985	97	5141	−59
1	0	4	0.458	18331		18044	287	18422	−91	19524	−1193
2	4	1	0.474	149		178	−29	198	−49	259	−110
4	2	−1	0.474	2828		2772	56	2825	3	2979	−151
2	0	−4	0.482	329		291	38	285	44	271	58
5	0	2	0.490	23387		23396	−9	23815	−428	24966	−1579
5	1	1	0.496	901		909	−8	917	−16	942	−41
1	5	−1	0.496	429		425	4	429	0	439	−10

(*b*) Agreement factors obtained for the three crystal models given in (*a*)

The first value refers to 26 weak reflections with $H < 0.5$ Å^{-1}, the second, in parentheses, to 102 weak reflections with $H < 0.73$ Å^{-1}.

	Neutral		$p(Be)\simeq 0.8$ $p(F)\simeq 0.7$ $p(Li)\simeq 0.6$		Ionic
$\Sigma(\lvert I_o - I_c\rvert) \times 10^{-1}$	433	(1569)	339	(1345)	2978 (4011)
$Q = \Sigma w(I_o - I_c)^2 \times 10^{-1}$	205	(1053)	137	(946)	1769 (2876)
$R(F)$	0.009	(0.009)	0.009	(0.009)	0.050(0.017)
$R(I)$	0.014	(0.015)	0.011	(0.012)	0.097(0.038)

butions of the atoms beyond the input map edges, was also set to 6 Å. An essential feature of the Hirshfeld approach is that it yields zero charge transfer for the promolecule density. In addition, it is relatively robust against small changes in the experimental details.

We now describe the results obtained from data set 1. Since our earlier analysis (Seiler & Dunitz, 1986*a*), the weak reflections have been re-examined and corrected for large multiple-scattering contributions. In addition, in the present analysis, the 280 weakest reflections ($1.0 < H < 1.8$ Å^{-1} and $I_o < 40$) were excluded from the difference synthesis because they contain a systematic error (see *Analysis of data*) and considerable noise. The errors in peak heights and atomic net charges, introduced by excluding reflections, are discussed below. The average standard deviation of the difference density, estimated as $[2\Sigma\sigma^2(F_o)]^{1/2}/V$ is about 0.01 e Å^{-3} for the remaining 1557 reflections with $H < 1.8$ Å^{-1}.

Fig. 2 shows sections roughly parallel to (011) through the deformation density of a chain of atoms. With respect to the neutral-atom procrystal model (Fig. 2*a*), excess density is concentrated around anions rather than around cations. The deformation-density peaks along Be—F and Li—F bonds amount to about 0.22 and 0.085 e Å^{-3}, respectively, and it appears that they are on the whole closer to F centers. The largest negative densities (~ -0.14 e Å^{-3}) occur at Be centers. Estimated atomic net charges are about +0.14 (1), +0.09 (1) and −0.08 (1) e for Be, Li and F atoms, respectively.

In the map derived from the ionic procrystal model (Fig. 2*b*), diffuse density appears around Be atoms. The apparent charge transfer (from F to Be atoms) is another indication that these crystals are

built neither from neutral atoms nor from ions but from intermediate entities. Compared with Fig. 2(*a*), deformation-density peaks along Be—F bonds are slightly increased (to about 0.25 e Å^{-3}), while those along Li—F bonds are slightly decreased (to a mean value of about 0.05 e Å^{-3}). Moreover, Li—F peak heights are less regular than those obtained from the neutral-atom model. Since the partitioning of the deformation density in program *CHARGE* is always based on neutral-atom stockholders, the charges based on Fig. 2(*b*) are not meaningful.

Difference-density maps and net charges were also derived from data set 2 [794 ($F_o - F_c$) coefficients with $H < 1.4$ Å^{-1}] because extinction and (remaining) multiple-scattering contributions are less severe. Fig. 3(*a*) shows a section roughly parallel to (110) through atoms based on the neutral-atom model. A corresponding map obtained from data set 1 (Fig. 3*b*) shows that the deformation-density features obtained from the two crystal specimens are very similar. In both maps diffuse density appears around anions rather than around cations (as observed in Fig. 2*a*); peak heights along Be—F and Li—F bonds, based on data set 2 are about 0.015 and 0.005 e Å^{-3} greater than those obtained from data set 1; corresponding net charges increase by 3 to 4 e.s.d.'s to +0.18 (1), +0.13 (1) and −0.11 (1) e for Be, Li and F atoms, respectively. Thus, the deformation-density results obtained from two data sets at 81 K indicate that covalent interactions, especially in the Be—F bonds, must be appreciable, in agreement with McGinnety's (1973) suggestions. The observed peak heights are about half of those found by Collins *et al.* (1983). A more quantitative description of the electron-density features in this crystal could be obtained from a static deformation-density map based on an atom-centered multipole expansion involving the two extreme reference models.

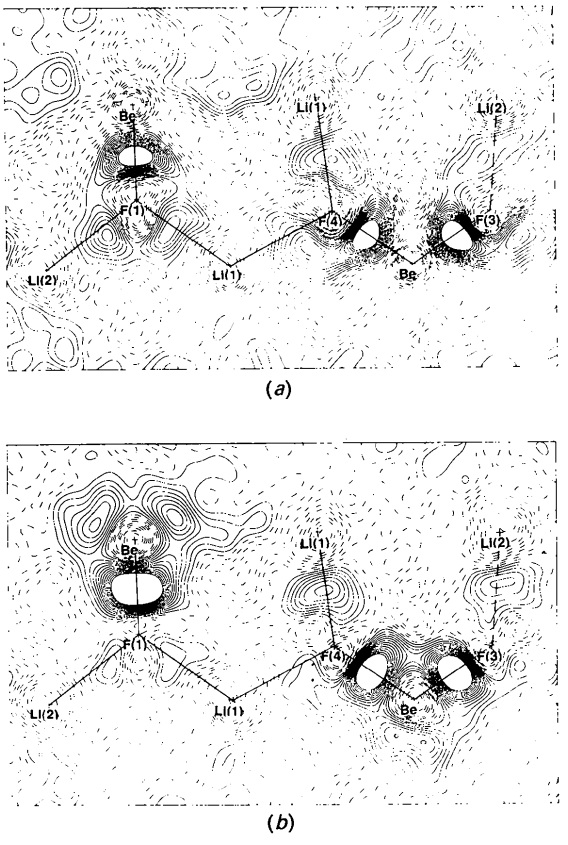

Fig. 2. Sections roughly parallel to (011) through the deformation density of a chain of atoms calculated with 1557 $F_o - F_c$ coefficients out to $H = 1.8$ Å^{-1}. (*a*) Based on the neutral-atom procrystal model *N*1; (*b*) based on the ionic model *I*1. In both maps contour levels are drawn at intervals of 0.01 e Å^{-3}: full lines for positive density; dot-dashed for zero; dashed for negative. Net charges derived from map (*a*) are +0.14 (1), +0.09 (1) and −0.08 (1) e for Be, Li and F atoms, respectively.

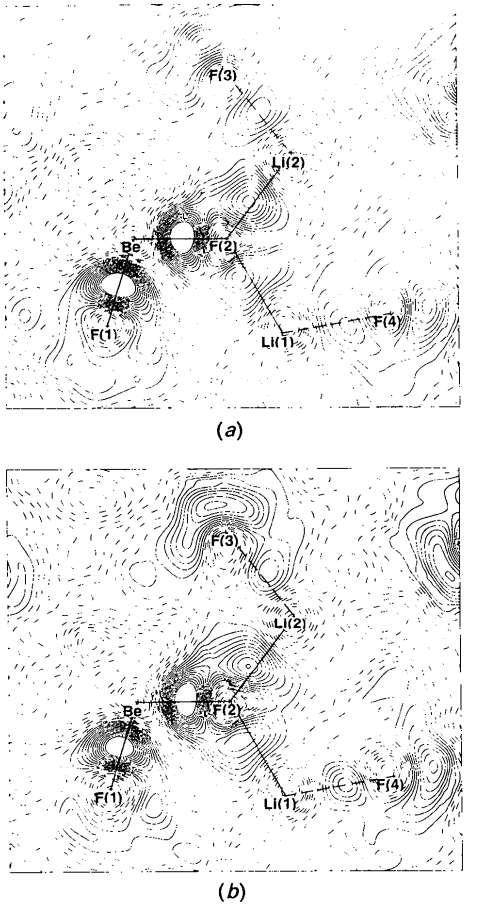

Fig. 3. Sections parallel to (110) through the deformation density of a chain of atoms obtained from (*a*) crystal 2 and (*b*) crystal 1. Both maps are based on the neutral-atom procrystal model *N*1 and 794 $F_o - F_c$ coefficients out to $H = 1.4$ Å^{-1}. Contour interval as for Fig. 2.

Estimation of the upper limit of (diffuse) charge transfer

Because of the diffuseness of the electron distribution involved in the possible charge-transfer process, it is not at all obvious what we should expect to see in a deformation-density map based on an inappropriate model. For example, for a hypothetical structure built of conventional spherical ions and a reference model built of neutral atoms, we can hardly expect to observe deficits of one and two electrons around Li and Be atoms, respectively, and corresponding accumulations of one electron around each of the F atoms. What is the upper limit of the observable (diffuse) charge transfer between cationic and anionic components in a crystal like Li_2BeF_4? To examine this question, we have made model-difference maps, by subtracting a neutral-atom promolecule density from a purely ionic one. Atomic parameters for the individual promolecules were taken from the least-squares refinements described above. The difference density, $\Delta\rho = \rho^{pro}(I1) - \rho^{pro}(N1)$, based on 67 $F_c - F_c$ coefficients with $H < 0.6$ Å^{-1} is shown in Fig. 4. Indeed, there are density deficits at Be and Li atoms and accumulations at F atoms but they are not pronounced. Peak heights at Be, Li and F centers are about -0.13, -0.01 and $+0.14$ e Å^{-3} and the corresponding estimated net charges (q_0) are only about $+0.39$ (1), $+0.18$ (1) and -0.19 (1) e, respectively. To test the reliability of such a procedure $\Delta\rho = \rho^{pro}(N1) - \rho^{pro}(I1)$ was also calculated (the details are not given here); corresponding q_0 values are reversed in sign and slightly smaller in absolute magnitude (by about 2 e.s.d.'s). The difference occurs because the scale factor differs slightly from one model calculation to the other. Hence, the net charges obtained from noninteracting approximately spherical pseudo atoms (ions) yield only about 19% of the ionic charges (Be^{2+}, Li^+, F^-). The main reason for this discrepancy is due to overlap of neighboring-atom densities. It is evident that negative difference-density components, centered around cations, and positive components, centered around anions, must partially cancel in the region of overlap. In a theoretical study of diatomic molecules, Maslen & Spackman (1985) came to a similar conclusion. They pointed out that with Hirshfeld's partitioning method the apparent loss of charge transfer in Li^+F^-, caused by such an effect, is about 0.4 e. Moreover, they found that there is an almost linear relationship between the loss of charge transfer and the internuclear distance (R), for R values between 1.5 and 4.5 a.u. In Li_2BeF_4, the loss is much more pronounced because each Li and Be atom is surrounded by a tetrahedron of F atoms and, in addition, the Li—F internuclear distances (see Table 2) are about 0.15 Å shorter than in Li^+F^-. Furthermore, the overlap increases with temperature, *e.g.* preliminary model calculations for Li_2BeF_4, based on room-temperature data, indicate that the observable charge transfer is about 10% lower than that determined at 81 K. A more detailed analysis of this problem, involving the temperature dependence, will be discussed in a subsequent paper.

Comparison of deformation densities and model-difference densities

A deformation density-map, based on data set 2, using only 67 Fourier coefficients out to $H = 0.6$ Å^{-1} is shown in Fig. 5. As in the model map (see Fig. 4), positive density occurs at F centers, and negative density at Be centers; the corresponding peak heights in the deformation-density map, however, are much lower. The difference density at Li centers is almost zero in both maps (~ -0.01 *e* Å^{-3}), as a result of the diffuseness of the Li (2*s*) electron. Estimated net charges are about $+0.14$ (1), $+0.11$ (1) and -0.09 (1) *e* for Be, Li and F atoms, respectively, *i.e.*

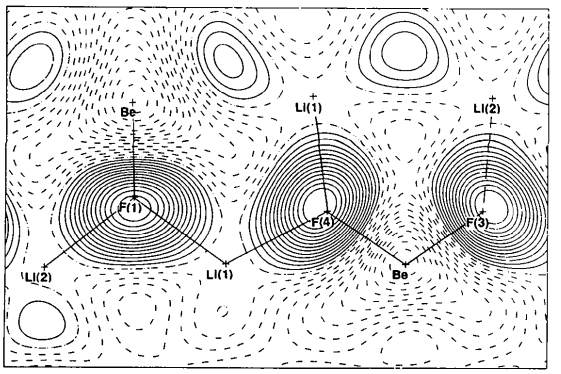

Fig. 4. Model-difference map, $\Delta\rho = \rho^{pro}(I1) - \rho^{pro}(N1)$, calculated with 67 Fourier coefficients out to $H = 0.6$ Å^{-1}. Contour interval as for Fig. 2.

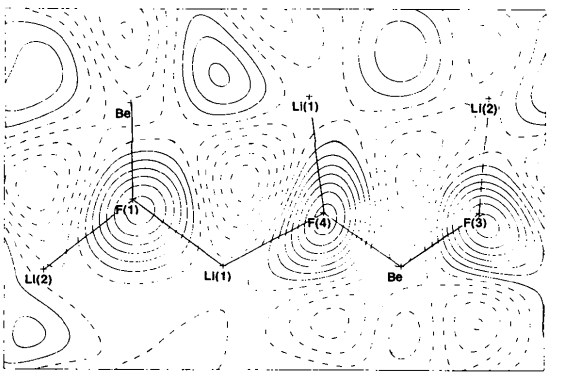

Fig. 5. Deformation-density map, $\Delta\rho = \rho^{mol} - \rho^{pro}(N1)$, based on crystal 2 and 67 Fourier coefficients out to $H = 0.6$ Å^{-1}. Contour interval as for Fig. 2.

they are about 20% smaller than corresponding q values derived with all Fourier coefficients out to $H = 1.4$ Å^{-1}.

Sections through F atoms, roughly perpendicular to Be—F and Li—F bonds (of the planes shown in Figs. 2, 4 and 5) show another feature of the electron density in this crystal. Fig. 6(*a*) shows the model difference density, $\Delta\rho = \rho^{pro}(I1) - \rho^{pro}(N1)$, based on 67 Fourier coefficients out to $H = 0.6$ Å^{-1}; (*b*) and (*c*) are deformation-density maps obtained from data set 1, based on 67 and 794 Fourier coefficients out to $H = 0.6$ and 1.4 Å^{-1}, respectively. In the model map, and to a lesser extent in the deformation-density maps, there is positive density around F centers. Moreover, the deformation-density maps (Figs. 6*b* and 6*c*) suggest that the F atoms are linked by diffuse density bridges (up to ~ 0.02 e Å^{-3}). It is difficult to say whether this residual density (also visible in corresponding maps of crystal 2) is centered around cations or around anions. Also, we do not know if this feature is real or due to an inadequate crystal model (neglect of anharmonic vibrations, disorder, inadequate extinction correction *etc.*). Note, however, that anharmonic vibrations are expected to be quite small at 81 K, since the thermal-expansion coefficient of Li_2BeF_4 crystals below 130 K is extremely small.

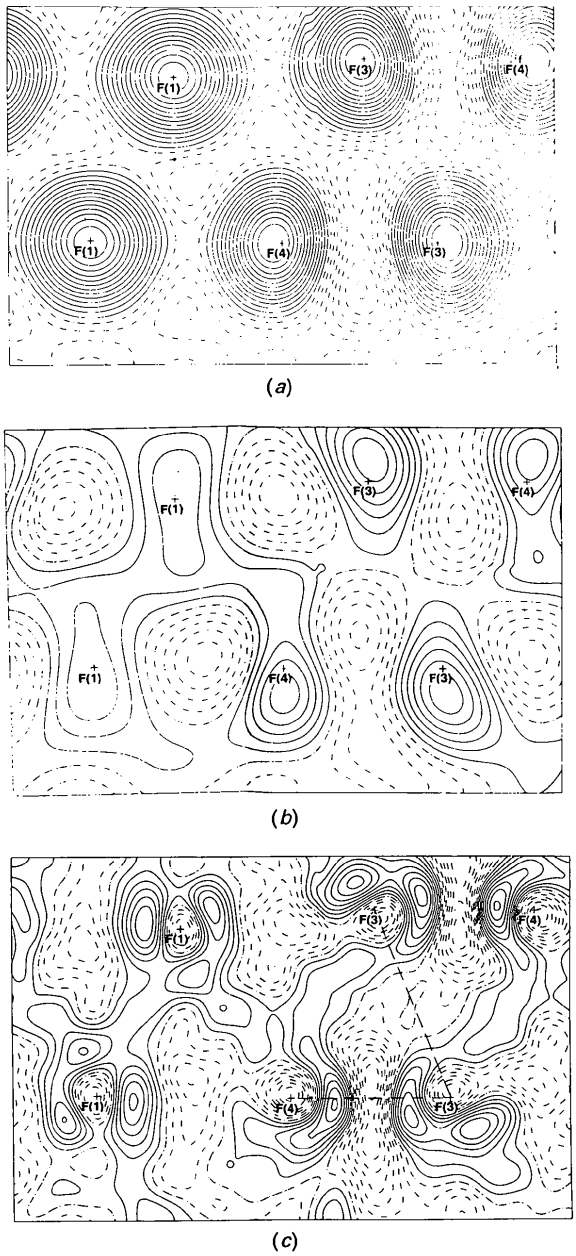

Fig. 6. Sections roughly perpendicular to Be—F and Li—F bonds (of the planes shown in Figs. 2, 4 and 5) through the difference density of F atoms. (*a*) $\Delta\rho = \rho^{pro}(I1) - \rho^{pro}(N1)$, calculated with 67 $F_c - F_c$ coefficients out to $H = 0.6$ Å^{-1}; (*b*), (*c*) deformation-density maps obtained from crystal 1, including 67 and 794 $F_o - F_c$ coefficients out to $H = 0.6$ and 1.4 Å^{-1}, respectively. Contour interval as for Fig. 2.

Ionicity coefficients from difference maps

At this point it seems useful to summarize the results on atomic charges. According to our model calculations, the diffuse charge transfer (q_0) between cationic and anionic components is only about 19% of formal ionic charge values, namely +0.39 (1), −0.19 (1) and +0.18 (1) e for Be, F and Li atoms, respectively; the corresponding atomic net charges (q) (average values of two crystal specimens) based on the neutral-atom reference model $N1$ are about +0.16, −0.094 and +0.109 e. Ionicity coefficients p ($p = 1$ for neutral; $p = 0$ for ionic), based on the ratio q/q_0, are 0.59, 0.50 and 0.39 for Be, F and Li atoms, respectively. Thus both types of analysis, in real and in reciprocal space, show that the degree of ionicity of the atoms in Li_2BeF_4 is increasing in the order Be < F < Li.

Systematic errors in peak heights and net charges

To assess the accuracy of our results we carried out various tests. Firstly, the series-termination effect was estimated for data set 1, by extending the cut-off value successively from $H = 1.8$ to 2.2 Å^{-1}. The maximum change in the (mean) Be—F and Li—F deformation-density peak heights lies within 0.02 e Å^{-3}. Atomic net charges based on the Hirshfeld partitioning method are even less sensitive, *i.e.* cut-off values between $H = 1.4$ and 2.2 Å^{-1} give almost identical q values (within 0.005 e).

Secondly, exclusion of the weakest reflections (with $I_o < 40$ and $H > 1.0$ Å^{-1}) from the difference synthesis reduces (mean) Li—F and Be—F peak heights by about 0.01 and 0.02 e Å^{-3}, respectively, while q values stay practically the same.

Thirdly, a scan-truncation error, as introduced in data set 1 mod (see *Experimental*) likewise has only an insignificant effect; Li—F and Be—F peak heights decrease by about 0.005 e $Å^{-3}$ on average and net charges increase by less than 0.01 e.

Fourthly, the influence of different extinction-correction models was examined for both data sets. A type 2 extinction correction [Becker & Coppens (1974) formalism with a Lorentzian mosaic-spread distribution] produces significantly lower peaks and net charges than a type 1 correction. For crystal 1, in which extinction is more severe (see *Extinction correction* section), the corresponding differences are as large as 50%, whereas for crystal 2 they are only about 10%. Moreover, peaks and troughs in the deformation-density map of crystal 1 based on a type 2 correction are quite distorted. There is no doubt that the applied type 1 correction is the better choice for all three crystal specimens, even though the least-squares results are not conclusive with regard to the extinction type.

How reliable are standard scattering curves?

So far, the reference models were based on standard scattering factors calculated at the Hartree–Fock level for isolated atoms. According to Hess *et al.* (1993) the Hartree–Fock approach is a reasonable approximation for the density of the atomic cores, but not necessarily for the density of the outer valence shells. Thus, some of the calculations were repeated with the scattering factors of Hess *et al.* (1993), in which electron correlation and crystal-field corrections for Li_2BeF_4 are considered. Before discussing the results, a short comparison of the different sets of scattering factors used here is required. The *f* curves obtained from configuration interaction (CI) calculations for Li^0, Li^+ and Be^{2+} are almost indistinguishable from those listed in *International Tables for X-ray Crystallography* (1974, Vol. IV). For *f* curves of Be^0 and F^0, Δf[CI minus self-consistent field (SCF)] is not more than about 1.2 and −0.5% at $H = 0.28$ and 0.4 $Å^{-1}$, respectively. Crystal-field effects in Li_2BeF_4 are at most significant for F ions. The scattering curve for F^-, corrected for electron correlation and crystal-field effects, gives a maximum Δf(CI + Watson potential minus SCF) of about 1.4% at $H = 0.38$ $Å^{-1}$. The close similarity is due to the fact that the two corrections partly cancel at low *H* values (see Hess *et al.*, 1993). According to the present results, (at least) Be and F atoms are far from 'ionic' and thus it is likely that the crystal-field correction, estimated with standard charge values (Be^{2+}, Li^+, F^-), is somewhat too large. Also, the electrostatic field acting on F^- (determined mainly by a single Be—F contact) is not spherical and the applied procedure, based on a spherical average, may lead to an additional uncertainty.

CI results

To distinguish between the different sets of scattering factors (and corresponding crystal models) of Hess *et al.* (1993), the following notation is used: *N*2 and *I*2 refer to neutral-atom and ionic scattering factors at the CI level and *I*3 refers to ionic scattering factors at the CI level in which a Watson potential is considered for F atoms.

With the new scattering curves, *p* coefficients derived in reciprocal space with data set 3 are virtually the same as those obtained with standard Hartree–Fock *f* curves, namely about 0.8, 0.7 and 0.6 for Be, F and Li atoms, respectively. The calculated intensities of the 26 model-sensitive reflections ($H <$ 0.5 $Å^{-1}$) based on the two extreme procrystal models are slightly larger. From *N*1 to *N*2 they increase by about 1.5% and from *I*1 to *I*3 by about 0.5% on average. The corresponding agreement factors are also slightly larger than those obtained from standard *f* curves.

Deformation-density maps, based on *N*2 and *I*3, are almost indistinguishable from corresponding maps shown in Figs. 2 and 3. Comparable peak heights along Be—F and Li—F bonds agree within about one contour; net charges (*q*) (average values of two crystal specimens) based on *N*2 are +0.167, −0.087 and +0.093 e for Be, F and Li atoms, respectively, *i.e.* they agree within 0.01 e with corresponding *q* values based on *N*1. Net charges (q_0) based on model difference maps $\Delta\rho = \rho^{pro}(I2) - \rho^{pro}(N2)$ and $\Delta\rho = \rho^{pro}(I3) - \rho^{pro}(N2)$ are about 15 and 25% of the ionic charge values (Be^{2+}, Li^+, F^-), respectively. In other words, inclusion of electron correlation alone increases the overlap among reference atoms slightly; inclusion of crystal-field effects (for F^-) reduces it. In view of the small differences observed relative to standard *f* curves (and with consideration that the applied crystal-field correction is probably too large), it would be difficult to claim that the new *f* curves provide a significant improvement.

I am grateful to Professors W. H. E. Schwarz, H. L. Lin, J. E. Niu and B. Hess for communicating their results prior to publication, to Dr Volker Gramlich for his help with the *XTAL* system and to Professor Jack D. Dunitz for his comments and improvements on an earlier version of the manuscript.

References

BECKER, P. J. & COPPENS, P. (1974). *Acta Cryst.* **A30**, 129–147.
BRAGG, W. L. (1927). *Proc. R. Soc. London Ser. A*, **113**, 642–657.
BRAGG, W. L., JAMES, R. W. & BOSANQUET, C. H. (1921). *Philos. Mag.* **42**, 1–17.
BRAGG, W. L. & ZACHARIASEN, W. H. (1930). *Z. Kristallogr.* **72**, 518–528.

BURNS, J. H. & GORDON, E. K. (1966). *Acta Cryst.* **20**, 135–138.
BUSING, W. R. (1972). *J. Chem. Phys.* **57**, 3008–3010.
CATLOW, C. R. A. & STONEHAM, A. M. (1983). *J. Phys. C*, **16**, 4321–4338.
COLLINS, D. M., MAHAR, M. C. & WHITEHURST, F. W. (1983). *Acta Cryst.* B**39**, 303–306.
DUNITZ, J. D., SCHWEIZER, W. B. & SEILER, P. (1983). *Helv. Chim. Acta*, **66**, 123–133.
HAHN, T. (1954). *Neues Jahrb. Mineral. Abh.* **86**, 1–65.
HESS, B., LIN, H. L., NIU, J. E. & SCHWARZ, W. H. E. (1993). *Z. Naturforsch. Teil A*. In the press.
HIRSHFELD, F. L. (1977). *Theor. Chim. Acta*, **44**, 129–138.
HIRSHFELD, F. L. & RABINOVICH, D. (1973). *Acta Cryst.* A**29**, 510–513.
LE PAGE, Y. & GABE, E. J. (1979). *Acta Cryst.* A**35**, 73–78.
MCGINNETY, J. A. (1973). *J. Chem. Phys.* **59**, 3442–3443.
MASLEN, E. N. & SPACKMAN, M. A. (1985). *Aust. J. Phys.* **38**, 273–287.
MATHIESON, A. MCL. (1982). *Acta Cryst.* A**38**, 378–387.
MATHIESON, A. MCL. (1984). *Acta Cryst.* A**40**, 355–363.
MATHIESON, A. MCL. (1988). *Aust. J. Phys.* **41**, 393–402.
SEILER, P. (1992). *Accurate Molecular Structures*, edited by A. DOMENICANO & I. HARGITTAI, pp. 170–198. Oxford Univ. Press.
SEILER, P. & DUNITZ, J. D. (1986*a*). *Helv. Chim. Acta*, **69**, 1107–1112.
SEILER, P. & DUNITZ, J. D. (1986*b*). *Helv. Chim. Acta.* **69**, 1187.
SEILER, P., SCHWEIZER, W. B. & DUNITZ, J. D. (1984). *Acta Cryst.* B**40**, 319–327.
STEWART, J. M. & HALL, S. R. (1990). Editors. *The XTAL System of Crystallographic Programs – User's Manual.* Univ. of Maryland, College Park, Maryland, USA.
STEWART, J. M., KRUGER, G. J., AMMON, H. L., DICKINSON, C. W. & HALL, S. R. (1972). The *XRAY*72 system – version of June 1972. Tech. Rep. TR-192. Computer Science Center, Univ. of Maryland, College Park, Maryland, USA.
ZACHARIASEN, W. H. (1926). *Nor. Geol. Tidsskr.* **9**, 65–73.

Acta Cryst. (1993). B**49**, 235–244

The Twin Structure of $La_2Ti_2O_7$: X-ray and Transmission Electron Microscopy Studies

BY HELMUT W. SCHMALLE, TIM WILLIAMS* AND ARMIN RELLER

Institute for Inorganic Chemistry, University of Zürich, Winterthurerstrasse 190, *CH*-8057 *Zürich, Switzerland*

ANTHONY LINDEN

Institute for Organic Chemistry, University of Zürich, Winterthurerstrasse 190, *CH*-8057 *Zürich, Switzerland*

AND J. GEORG BEDNORZ

IBM Research Division, Zürich Research Laboratory, CH-8803 *Rüschlikon, Switzerland*

(*Received* 15 *November* 1991; *accepted* 23 *September* 1992)

Abstract

$La_2Ti_2O_7$, $M_r = 485.613$, monoclinic, $P2_1$, $a = 7.812\,(2)$, $b = 5.5440\,(7)$, $c = 13.010\,(2)$ Å, $\beta = 98.66\,(1)°$, $V = 557.0\,(4)$ Å^3, $Z = 4$, $T = 298$ K, $D_x = 5.790$ Mg m^{-3}, λ(Mo $K\alpha$) = 0.71073 Å, $\mu = 17.86$ mm^{-1}, $F(000) = 856$. The crystals are twinned. The twin I and twin II intensities are superimposed in reciprocal-lattice layers with h even. The **a*** and **b*** axes of the twin components run antiparallel. The angle between $\mathbf{a}^*_{\text{twin I}}$ and $\mathbf{a}^*_{\text{twin II}}$ is 17.12°. The twinning operation has been identified to be a mirror plane perpendicular to the **c*** direction affecting only the oxygen positions in the structure: La and Ti atoms lie on an orthorhombic sublattice unchanged by the twinning. The structure refined on $|F|^2$ to $R = 0.040$, $wR = 0.085$ for 7972 observed reflections with $I > 3\sigma(I)$. The refinement was carried out by inclusion of the contributions from the two twin elements simultaneously, with the use of appropriate matrices to relate the atomic coordinates and reflection indices of each of the twin elements. The twin volume fraction was also refined and gave $\alpha = 0.1108\,(3)$ as the volume fraction of twin I. The enantiomorphs in twin I and twin II have been shown to be opposite by refinement, on $|F|$, of the enantiopole, or Flack's x, parameter against reflection data that had been separated into separate sets for each twin element. Subsequently, several refinements, on $|F|$, of the twinned data set with the use of all possible combinations of enantiomorphs of each twin element yielded the best R/wR values (0.040 and 0.056) when the twin components contained opposite enantiomorphs. The general features of the structure determined by Gasperin [*Acta Cryst.* (1975), B**31**, 2129–2130] could be confirmed: the twins comprise distorted (4 + 1 + 1) TiO_6 octahedra sharing vertices to form infinite perovskite-like layers three octahedra thick, bound by crystallographic

* Author to whom all correspondence should be addressed. Present address: JASCO International Co. Ltd., 4–21 Sennin-cho 2-chome, Hachioji City, Tokyo 193, Japan.

0108-7681/93/020235-10$06.00